BioEnergy Research (2019) 12:1077–1089
https://doi.org/10.1007/s12155-019-10037-2

# Pyrolysis Kinetics Using TGA and Simulation of Gasification of the Microalga *Botryococcus braunii*

Andrés A. Arbeláez[1] · Néstor D. Giraldo[1] · Juan F. Pérez[2] · Lucía Atehortúa[1]

Published online: 21 August 2019


## Abstract

Microalgal biomass has been widely investigated as a source of renewable energy, but currently, some alternatives are not economically competitive. Thermochemical conversion of biomass is an alternative way to transform their organic compounds into liquid and gaseous fuels. The aim of this work is twofold; first, the pyrolytic process of the microalga *Botryococcus braunii* (*BB*) by thermogravimetric analysis, as well as the relevant reaction kinetic constants and related activation energies, is assessed. Secondly, a sensitivity analysis of the biomass gasification process with air using a thermochemical model was conducted to predict the composition of a syngas as a function of the biomass moisture content and the biomass/air ratio. The results showed that *BB* biomass is composed mainly of carbon (62.4 wt.%) with volatile solids of 84 wt.%, while the fixed carbon represents around 7 wt.%. Additionally, observed values for heating (27.86 MJ $kg^{-1}$) and activation energy (~ 110 kJ $mol^{-1}$) were different from other algal feedstocks due to the capacity of accumulation of liquid hydrocarbons of this. On the other side, the gasification process showed it was found that the moisture content in the biomass and biomass/air ratio variables are key parameters for reaction temperature and producer gas composition. Accordingly, with a suitable combination of these variables, it is possible to obtain a syngas composed of gaseous species with high energy content (CO, 18 vol.%; $H_2$, 17 vol.%; and $CH_4$, 2 vol.%.), which can be transformed through processes such as Fisher-Tropsch process into liquid biofuels such as kerosene or gasoline.

**Keywords** Microalgal biofuels · Biomass thermochemical conversion · *Botryococcus braunii* · Pyrolysis · Biomass gasification

## Introduction

Fossil fuels are the basis of the energy and production infrastructure on the planet; however, these are a finite resource whose processing, use, and depletion represent environmental and social concerns that are currently of global interest. Consequently, the development of technologies to use renewable sources as fuel (i.e., feedstocks) is a key step in the transition from the oil-based model to a more diverse and environmentally responsible model [1]. In the path of this transition, new alternatives have arisen such as the use of biomass as an input to produce solid, liquid, and gaseous fuels compatible with current energy technologies [2–4]. Biomass spans a broad range of materials derived from plants such as wood, grains, forage, and agroindustry wastes as well as the mass produced by macroalgae and microalgae. Recently, the biomass produced by microalgae has attracted a special attention as it is a fast-growing aquatic photosynthetic microorganism that can be produced simply and economically. Microalgae biomass is interesting not only because of its potential in terms of energy but also because it presents the possibility of establishing a biorefinery that produces energy and higher value products such as proteins and bioactive compounds [5]. One of the most suitable microalgae species to be used as raw material for energy purposes is *Botryococcus braunii*, a green microalga known for its ability to produce and accumulate significant amounts of liquid hydrocarbons suitable to produce biofuels [6].

Microalgal represents important benefits as a source of biomass compared to other conventional sources. As photosynthetic microorganisms, the primary carbon source is carbon dioxide, with 1.0 kg of algal biomass produced from approximately 1.8 kg of $CO_2$ [7, 8]. Additionally, it is possible to obtain a high yield in a wide spectrum of environments and

✉ Andrés A. Arbeláez
alonso.arbelaez@udea.edu.co

[1] Grupo de Biotecnología, Instituto de Biología, Facultad de Ciencias Exactas y Naturales, Universidad de Antioquia UdeA, Calle 67 No. 53-108, Medellín, Colombia

[2] Departamento de ingeniería mecánica Grupo de Manejo Eficiente de la Energía (GIMEL), Facultad de ingeniería, Universidad de Antioquia UdeA, Calle 67 No. 53-108, Medellín, Colombia

simple cultivation systems such as freshwater or seawater ponds without competing for arable land or compromising food security [9–11].

Thermochemical conversion of microalgae is an attractive pathway to transform biomass into different forms of useful energy [12]. These processes mainly include direct combustion to generate heat and electricity, as well as pyrolysis and gasification to produce liquid and gaseous fuels which are suitable for engines and turbines [13]. Pyrolysis plays an important role in thermochemical conversion processes, being the chemical starting point of gasification and combustion processes, which can be divided into two consecutive scenarios that involve the thermal decomposition of biomass, through the devolatilization of the most volatile compounds and a slow heterogeneous conversion to coal [13].

A number of authors have reported pyrolytic kinetics studies in different types of microalgae [14–18], showing large differences in pyrolytic behavior depending on its composition. The main components of microalgae including carbohydrates, lipid, and protein are easily degraded at temperatures between 200 and 450 °C with heating rates of 40 °C. The carbohydrates are easily degraded at temperatures between 220 and 350 °C, while proteins degrade between 300 and 400 °C and lipids require higher temperature mainly between 320 and 420 °C [18]. The cell walls of green algae are mainly composed of polymers like cellulose-pectin complexes, glycoproteins, and other carbohydrates to a lower extent [19, 20]. These components are easier to pyrolyze compared to those reported for lignin, which is the main compound of the woody raw material commonly used for thermochemical conversion processes [21, 22]. In contrast, pyrolytic studies on macroalgae show similar results in carbohydrate degradation peaks, mainly composed of polysaccharides such as xylan and dextran and a large amount of water-soluble polysaccharides, including rhamnose, xylose, and uronic acid, where heating rates of 20 °C show degradation peaks between 250 and 300 °C [23]. The composition of the pyrolysis gas and its properties depend directly on the chemical structures of the biomass components, for example hemicellulose, with higher carboxyl content, accounts for a higher $CO_2$ yield, while cellulose displays a higher CO yield, mainly attributed to the thermal cracking of carbonyl and carboxyl, and lignin releases out much more $H_2$ and $CH_4$ due to high presence of aromatic ring structures and methoxyl groups.

Biomass gasification is considered the most promising process with the best cost/benefit ratio for the conversion of biomass into energy [24]. Gasification is a thermochemical conversion process of solid materials composed mostly of carbon (such as biomass) into syngas. The syngas is mainly composed of hydrogen, carbon monoxide, carbon dioxide, and methane [25, 26]. The process performance depends on the applied gasification conditions [27]. Some authors have reported the use of microalgae as an alternative in the production of bioenergy through processes such as pyrolysis [16] and gasification [11], finding that it is possible to convert the marine microalga *Nannochloropsis gaditana* into syngas via gasification processing, obtaining a product mainly composed of $H_2$ (50%) and CO (35%) [28]. On the other hand, product analysis of different microalgal biomass shows that is possible produce alkane compounds with 9-octadecyne ($C_{18}H_{34}$) from *Chlorella sorokiniana,* when it is subjected to the pyrolysis process [29]. Moreover, the gasification process shows significant potential for the production of biofuels. For instance, it has been found that using *Nannochloropsis oculata* in fixed bed reactor easily obtains syngas composed mainly of $H_2$ (50%), $CH_4$ (10%), and CO (6%) with a carbon conversion of 70% [30].

The chemical, physical, energy, and thermochemical properties of biomass used as feedstock for thermochemical processes affect the reactor design [31]; in the same way, the reactor design affects the process performance for a specific biomass [32]. Therefore, in this work, the pyrolysis kinetics using TGA of the microalga *Botryococcus braunii* is analyzed, whose reaction kinetic mechanism supports the design of gasifiers in further stages [31]. Likewise, the thermodynamic limits of the gasification process of *Botryococcus braunii* are calculated by simulating the gasification process to contribute to pathways of energy valorization of this algal biomass, which model estimates the maximum expected thermodynamic performance of the thermochemical process using as feedstock this microalga.

## Materials and Methods

### Microalgal Biomass Production and Chemical Characterization

The green algae strain used in this work was *Botryococcus braunii* 572 from the culture collection of the University of Texas (UTEX). *B. braunii* was incubated in a stirred tank reactor with a working volume of 10 L in continuous mode with a dilution rate 0.11 $d^{-1}$, fed with modified medium based on $BG_{11}$, and illumination was provided by LED lamps (Cold white 6500 K) at a mean photon flux density of 960 μmol $m^{-2}$ $s^{-1}$ [33]. The harvested biomass was subjected to centrifugation at 15000*g* for 10 min, discarding the supernatant and performing 3 washes to reduce the salt content. Then, the harvested biomass was lyophilized and stored in vacuum.

The content of crude totals for protein, carbohydrates, and lipids was determined by the Kjeldehl method (factor of 6.25), the phenol-sulfuric acid method, and a modified method reported by Bligh and Dyer (1959) [34], respectively. The ultimate analysis was carried out in LECO model Truspec Micro elemental analyzer, using the method ASTM D-5373-08

(2012), while the proximate analysis was performed in TGA Q500 V20.13 Build 39 equipment using the ASTM D5142 modified methodology reported by Ceylan and Kazan (2015) [35]. The moisture content was determined with an isothermal process at 120 °C in a moisture analyzer. The volatile material content was determined by heating the sample to 800 °C under an inert $N_2$ atmosphere, and maintaining the temperature until constant mass observed. Then, air was injected during isotherm at 800 °C to oxidize the sample (fixed carbon). The ash content was determined by residue after oxidation. The biomass higher heating value (HHV) was estimated according the standard ASTM E144-14, where ~ 2 g of dry biomass was used in jacket pump calorimeter 1341 Parr model 2901EB. The lower heating value (LHV) was calculated from the HHV and hydrogen content [29] (Table 1).

## Thermogravimetric Analysis

The analysis of the thermal degradation of biomass samples was carried out using a TGA Q500 V20.13 Build 39. During the pyrolysis process, the samples were pre-treated at 110 °C to remove moisture, then the temperature was brought to 800 °C at four different constant heating rates of 10, 20, 30, and 40 °C $min^{-1}$. A nitrogen flow at 60 mL $min^{-1}$ was supplied as carrier gas. The loss of mass was expressed as a function of temperature. The rate of weight loss (dX/dt) for the biomass was recorded and used to plot the thermogravimetric analysis (TGA) and derivative thermogravimetry (DTG).

## Kinetic Pyrolysis Model

Non-isothermal method was carried out in the thermobalance, and the mass loss was expressed as a function of temperature. According to Vo et al. (2017) [14], the rate of degradation or thermal conversion dα/dt, is a linear function of temperature, and constant $k$ is dependent on temperature, with a temperature-independent conversion function, $f(\alpha)$:

The kinetics of pyrolysis could be described as:

$$\frac{d\alpha}{dt} = kf(\alpha) \tag{1}$$

The mass loss ratio ($\alpha$) can be calculated as follows:

$$\alpha = \frac{W_0 - W}{W_0 - W_\infty} \tag{2}$$

Where $W_0$ is the initial mass of the sample, $W$ is the sample mass at the time $t$, and $W_\infty$ is the final mass at the end of the thermogravimetric analysis.

The reaction rate, $k$, was represented as the Arrhenius equation:

$$k = A\exp\left(-\frac{E}{RT}\right) \tag{3}$$

Where $A$ is a pre-exponential factor ($min^{-1}$), $E$ is the activation energy (J $mol^{-1}$), $R$ is the gases constant (J $mol^{-1}$ $K^{-1}$), and $T$ is absolute temperature (K). Combining Eqs. 2 and 3, we have:

$$\frac{d\alpha}{dt} = A\exp\left(-\frac{E}{RT}\right) f(\alpha) \tag{4}$$

If the heating rate is constant, $\beta = dT/dt$, which can be inserted in Eq. 4 as follows:

$$\frac{d\alpha}{dT} = \frac{A}{\beta}\exp\left(-\frac{E}{RT}\right) f(\alpha) \tag{5}$$

Where $\alpha$ is the fractional conversion, $T$ is the kelvin temperature, $\beta$ is the heating rate, $A$ is the pre-exponential factor, $E$ is the activation energy, $R$ is the gas constant, and $f(\alpha)$ is the temperature-independent function of conversion related to the decomposition mechanism.

Equation 5 can be linearized by integration, which can be expressed as

$$\int_0^\alpha \frac{d\alpha}{f(\alpha)} = \frac{A}{\beta}\int_{T_0}^{T} \exp\left(\frac{-E}{RT}\right) dT \tag{6}$$

Here $G(\alpha)$ is the integrated form of the function $f(\alpha)$

$$G(\alpha) = \int_0^\alpha \frac{d\alpha}{f(\alpha)} \tag{7}$$

The linearized integrated equation form can see in the following expressions:

Kissinger–Akahira–Sunose (KAS) Equation [36].

$$\ln\left(\frac{\beta}{T^2}\right) = \ln\frac{AR}{E_a G(\alpha)} - \frac{E_a}{RT} \tag{8}$$

Flynn-Wall-Ozaka (FWO) Equation [37].

$$\ln(\beta) = \ln\left(\frac{0.0048\, AE_a}{RG(\alpha)}\right) - 1.016\frac{E_a}{RT} \tag{9}$$

**Table 1** Raw biomass characterization

| Proximate analysis (wt.%) | | Ultimate analysis (wt.%, dry-ash-free) | | Composition analysis (wt.%) | |
|---|---|---|---|---|---|
| Volatile material (VM) | 83.9 | C | 62.4 | Crude protein | 20 |
| Fixed carbon (FC) | 6.7 | H | 8.7 | Crude lipid | 44 |
| Moisture (M) | 4.6 | O | 21.6 | Carbohydrate | 31 |
| Ash (CN) | 4.8 | N | 6.5 | | |
| | | S | 0.8 | | |
| | | C:O molar ratio | 3.85 | | |
| | | O:C mass ratio | 0.35 | | |
| | | O:C molar ratio | 0.26 | | |
| Molecular formula | $CH_{1.66}N_{0.09}O_{0.26}S_{0.005}$ | | | | |
| HHV (MJ/kg, dry basis) | 27.86 | | | | |
| LHV (MJ/kg, dry basis) | 24.73 | | | | |

With a given value of conversion rate, plots of $\ln(\beta/T^2)$, $\ln(\beta)$ versus 1/T give straight lines with slopes $-E_a/R$ and $-1.016E_a/R$, with subsequent determination of activation energy ($E_a$). Substituting the value $E_a$ and the mechanism function $G(\alpha)$ back into Eqs. (4) and (5) in conjunction with $T$ and $\alpha$ allows ln$A$ to be calculated [17].

## Simulation of the Gasification Process

The gasification simulation process was performed using the model developed by Melgar et al. (2007) [38]. This model expresses the reactions of the gasification process in terms of mass and energy balances. This model allows to predict the composition of the "producer gas" (PG) or synthesis gas (syngas) and the reaction temperature of the gasification process. Therefore, as a function of the response variables of the model and biomass composition, it is possible to determine other important parameters such as lower heating value ($LHV_{PG}$) and engine fuel quality (EFQ) of the producer gas [38, 39]. These parameters define the quality of the PG fuel for applications in internal combustion engines. Therefore, the model is a useful tool to simulate the composition of the PG depending on the biomass type, the moisture content ($h$), and the fuel/air equivalence ratio ($F_{rg}$) [38, 39].

The input parameters required by the model are the ultimate analysis of the biomass, the moisture content, and the heating value. These are used to determine the elemental formula of biomass ($C_nH_mO_pN_qS_r$), and its molar water content [38]. Accordingly, the fuel/air ratio can be estimated under stoichiometric conditions using Eq. 11. Therefore, using the calculated stoichiometric parameter ($F_{stq.bms}$), the relationship between the actual fuel/air equivalence ratio used in the simulation ($F_{rg}$) and the stoichiometric combustion air can be established (Eq. 12). With these two parameters, the molar amount of real air is estimated (Eq. 13). A detailed procedure for the solution of the model and the auxiliary equations is reported by Pérez et al. (2016) [39].

$$CH_mO_pN_qS_r + wH_2O + x(O_2 + 3.76N_2) \rightarrow aCO + bCO_2 + cH_2 + dCH_4 + eH_2O + fN_2 + gO_2 + iSO_2 \quad (10)$$

$$F_{stq.bms} = \frac{1\text{mol}_{bms}\cdot(1 + m + 16p + 14q + 32r)(\text{kg/kmol})}{\left(1 + \frac{m}{4} + \frac{r}{2} - \frac{p}{2}\right)\text{mol}_{air}\cdot M_{air}(\text{kg/kmol})} \quad (11)$$

$$F_r = \frac{(\text{m}_{bms}/\text{m}_{air})_{actual}}{F_{stq.bms}} \quad (12)$$

$$X = \frac{1}{F_r F_{stq.bms}} \quad (13)$$

$$C + 2H_2 \leftrightarrow CH_4$$
$$\therefore K_1 = \frac{(P_{CH_4}/P_0)}{(P_{H_2}/P_0)} = \frac{dn_t}{C^2} \quad (14)$$

$$CO + H_2O \leftrightarrow CO_2 + H_2$$
$$\therefore K_2 = \frac{(P_{CO_2}/P_0)(P_{H_2}/P_0)}{(P_{CO}/P_0)(P_{H_2O}/P_0)} = \frac{bc}{ae} \quad (15)$$

$$T_{k+1} = T_k + \frac{h_{react} - h_{prod}(T_k)}{c_{p.prod}(T_k)} \quad (16)$$

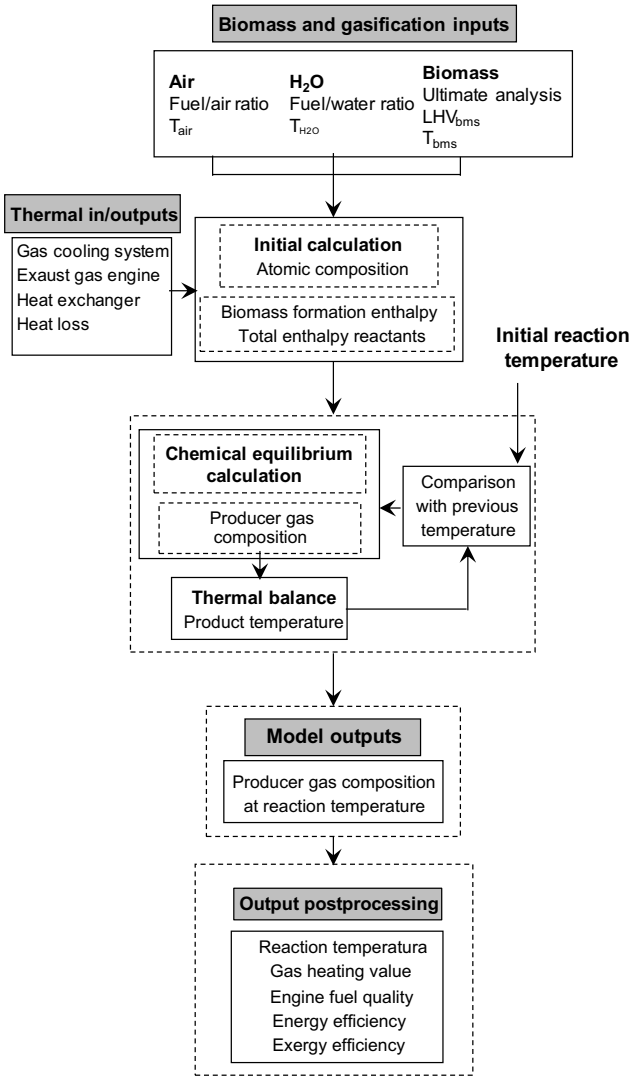


**Fig. 1** Block diagram of structure to solve the model

The simulation plan was conducted by varying the moisture content of the *Botryococcus braunii* microalga between 0.0 and 50 wt.%, and varying the fuel/air equivalence ratio from 1.0 (stoichiometric combustion) to 5.0 (gasification). The main parameters to be analyzed in the simulation of the gasification process were the producer gas composition in %vol. ($CH_4$, $H_2$, $CO_2$, and CO), as well as the $LHV_{PG}$, the EFQ, and process temperature.

### Model Structure

In Fig. 1, it is shown the block diagram that describes the structure necessary to solve the model. In the first stage (biomass and gasification inputs), moisture and ultimate analysis of biomass are calculated from the substitution formula of biomass and molar quantity of water. Real air molar quantity is calculated from fuel/air equivalence ratio, and total enthalpy of reactants is estimated.

In the second stage, producer gas composition is calculated by the Newton-Raphson method to solve the nonlinear equations system. Subsequently, reaction temperature is calculated by equalizing enthalpy of reactants (biomass, moisture, and air) and products (producer gas). Calculated temperature is the input for iterative calculation of producer gas composition until the chemical and thermal equilibria are reached. Therefore, thermodynamic parameters that characterize the thermochemical process are calculated with final producer gas and biomass compositions (ultimate analysis and heating value). Additional information related to the model is presented in detail in previous works [40].

## Results and Discussion

### Thermogravimetric Analysis

#### Thermal Degradation Process

The trends in weight loss curves obtained during TGA show the physical and chemical structural changes occurring during the thermal conversion. Differential thermogravimetry (DTG) curve indicates main devolatilization stages more clearly. TG and DTG curves of *BB* at four different heating rates from 100 to 700 °C are depicted in Fig. 2.

The start of biomass thermal degradation is linked to the decomposition of the most thermo-sensitive materials, which is reflected in a change in the mass of the sample (Fig. 2a). Two zones could be identified in Fig. 2b with two strong peaks similarly with the previous published work [16, 41, 42]. The first zone corresponds to the initial peak (250–350 °C) where compounds such as carbohydrates and proteins suffer from different decomposition mechanisms such as depolymerization, decarboxylation, and cracking [14, 18], this being the main stage of weight loss, reaching 50% of the total loss. The second zone shows a second strong peak corresponds to the lipid devolatilization (380–480 °C) [14, 18].

Some authors report that different microalgae species have different decomposition zones and different decomposition profiles, although they are mainly composed of carbohydrates, proteins, and lipids, due carbohydrates, proteins, and lipids include many types of subspecies, different subspecies of these main components may lead to different decomposition profiles [43]. For example, there was only one DTG peak for the pyrolysis of the microalga *Dunaliella tertiolecta* [16], *Hapalosiphon* sp. [43], *Tetraselmis* sp. [35], or seaweeds *Enteromorpha prolifera* [44] and *Enteromorpha clathrate* [45], because they have a low amount of lipids and the corresponding peak is not noticeable. In contrast, two DTG peaks were observed for the microalga *Nannochloropsis oculata* [35], *Aurantiochytrium* sp. [14], and *Chlorella sorokiniana* [18] and more than two DTG peaks were observed for *BB* in

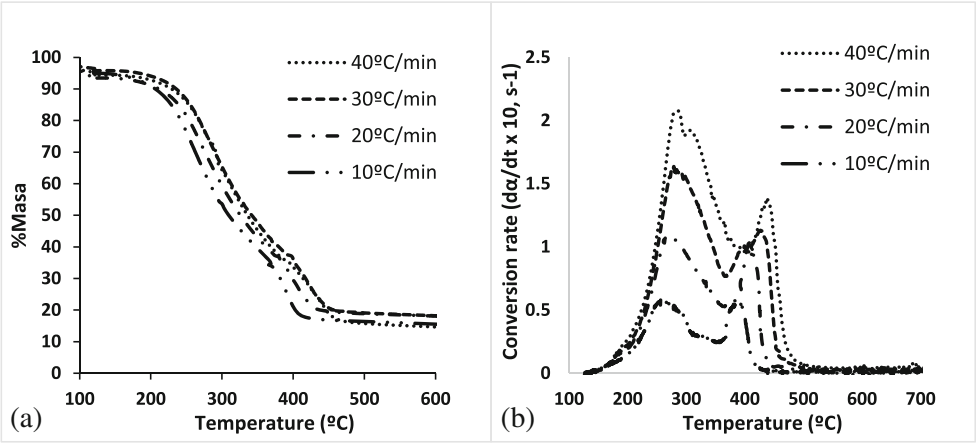


**Fig. 2** Thermal degradation process. **a** Thermogravimetric curves-TGA. **b** Differential thermogravimetric curves—DTG

this study. In fact, on the DTG curve of *BB*, three inflection points were observed at 290, 315, and 450 °C, which indicates that the two weak peaks were concealed by the main decomposition peak due to the carbohydrate and protein content of biomass (21% and 31% respectively) and a third strong peak which can be explained by considering the fact that the microalgae *Botryococcus braunii* is composed in a large amount of lipids reaching in this study 44%, which are reported to be rich in unsaturated linear chain of hydrocarbons [6, 46].

## Effect of Heating Rate

The shape TGA curves did not change with the heating rate for *BB*. However, it can be observed in Fig. 2b that the whole weight losses during the pyrolysis process for *BB* were shifted to higher temperature zones with increasing the heating rates from 10 to 40 °C $min^{-1}$. It is well known that the maximum conversion rate is affected by the heating rate [29, 35, 47], typical for all non-isothermal experiments; thus, the maximum conversion increases with increasing heating rate [14] because the temperature differential between the surface and the core increases rapidly generating a gradient that favors the transfer of heat even though the biomass has a high thermal resistance [16, 17]. The main reason is the limited capacity of microalgal biomass to conduct heat, producing temperature gradients across the radius of the biomass [16]. Therefore, the behavior of mass loss varies with heating rates, causing an initial decomposition on the surface of the material, with a subsequent reaction chain that decomposes the rest of the internal material at high speeds due to the accumulated energy [16, 17].

## Kinetic Analysis

Different conversion rates were chosen at different heating rates and temperatures to determine the activation energy of the samples. From Eqs. 8 and 9, the parameters $ln(\beta/T^2)$, $ln(\beta)$ vs $(1/T)$ are depicted, and an initial trend is observed. From the data, the kinetic parameters were calculated assuming a reaction order of 1 in different conversion degrees. In Fig. 3, the family of apparent parallel lines can be observed, which can be visualized for each degree of conversion analyzed. It can be found the activation energy in seven different conversion degrees for *BB*.

Table 2 shows the distribution of activation energies Ea and the correlation coefficients ($R^2$) of fitted equations obtained by means of the KAS and FWO method for various degrees of microalgal biomass conversion, as well as each respective pre-

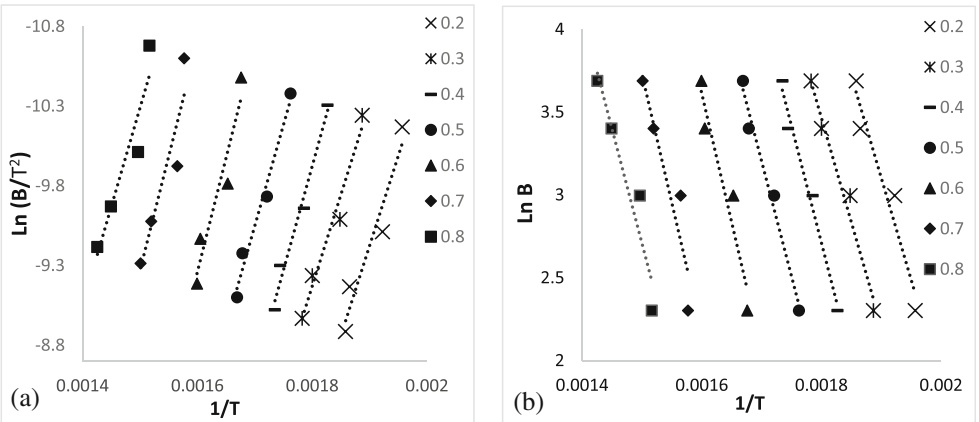


**Fig. 3** Graphs for the determination of activation energies at different conversion values α using the KAS (**a**) and FWO (**b**) methods

**Table 2** Activation energies obtained for different conversion values

| Conversion degree (α) | KAS method | | | | FWO method | | | |
|---|---|---|---|---|---|---|---|---|
| | Slope | Activation energy Ea (kJ mol$^{-1}$) | Coef. Corr ($R^2$) | Pre-exponential factor Ln A (min$^{-1}$) | Slope | Activation energyEa (kJ mol$^{-1}$) | Coef. Corr ($R^2$) | Pre-exponential factor Ln A (min$^{-1}$) |
| 0.2 | − 11,289 | 93.86 | 0.9336 | 19.28 | − 12,339 | 97.55 | 0.9439 | 20.13 |
| 0.3 | − 11,480 | 95.44 | 0.9703 | 19.24 | − 12,570 | 99.38 | 0.9752 | 20.10 |
| 0.4 | − 13,009 | 108.16 | 0.9775 | 21.26 | − 14,133 | 111.74 | 0.9809 | 22.02 |
| 0.5 | − 12,706 | 105.64 | 0.9760 | 19.92 | − 13,872 | 109.67 | 0.9799 | 20.75 |
| 0.6 | − 14,307 | 118.95 | 0.9141 | 21.37 | − 15,529 | 122.77 | 0.9262 | 22.11 |
| 0.7 | − 14,316 | 119.02 | 0.8611 | 20.10 | − 15,615 | 123.45 | 0.8807 | 20.91 |
| 0.8 | − 12,385 | 102.97 | 0.8980 | 17.14 | − 13,745 | 108.67 | 0.9158 | 18.13 |
| Average | | 106.29 | | | | | 110.46 | |

exponential factor. During the initial stage of pyrolysis, the activation energy increased progressively from 93.86 to 119.02 kJ mol$^{-1}$ as the degree of conversion increased from 20 to 70%. Thereafter, the activation energy rapidly decreased, reaching 102.97 kJ mol$^{-1}$ at a point where approximately 80% of the biomass was decomposed. The average apparent activation energy of *Botryococcus braunii* degradation was 106.29 and 110.46 kJ mol$^{-1}$ for KAS and FWO methods respectively.

It is observed that the energies obtained are comparable between the methods used, and that the energy range goes from 90 to 120 kJ mol$^{-1}$ depends on the degree of conversion required and pre-exponential factor is very similar in both methods. It can be observed that the activation energy required for the degrees of conversion (α) between 0.2 and 0.5 (proteins and carbohydrates mainly) has similar values to those required by the degrees of conversion between 0.6 and 0.9 (mainly lipids), which means that the lipids do not influence on increase of the average activation energy of the microalgal biomass. Similar results were obtained by Vo et al. (2017) [14], where degrees of conversion corresponding to proteins and carbohydrates of *Aurantiochytrium* obtained higher values of activation energy than those reported for lipids, whose average value is greater than that obtained in the present study (118.54 kJ mol$^{-1}$). A low activation energy means that the biomass requires low energy to break the chemical bonds between its atoms and initiate a reaction chain of devolatilization leading to increase the global efficiency of the thermochemical process [35, 47]. The activation energies, found in this study for *B. braunii*, are lower than those reported in other works with microalgae and raw materials used for the production of bioenergy [29, 48, 49] which could significantly reduce the operation cost for its pyrolysis.

Li et al. (2011) [17] investigated the kinetic and pyrolysis characteristics of three types of red algae *Pophyra yezoensis, Plocamium telfairiae harv*, and *Corallina pilulifera*. They found activation energies of 154, 244, and 250 kJ mol$^{-1}$ respectively. On the other hand, Ceylan et al. (2015) [35] investigated the behavior and kinetics of the pyrolysis process of microalgae *Nannochloropsis oculata* and *Tetraselmis* sp through a non-isothermal thermogravimetric study. They found that high activation energies are required for both microalgae with values of 152.2 kJ mol$^{-1}$ and 334 kJ mol$^{-1}$, respectively. These values are greater than those in the study presented here. However, this variation could be attributed to the differences of biochemical characteristics of the microalgae biomasses compared. Liu et al. 2012 [47] investigated the pyrolytic behavior of *Botryococcus braunii* and *Hapalosiphon* sp. through a non-isothermal thermogravimetric study using original biomass, residual biomass after oil extraction, and oil extracted from original biomass. They found activation energies from original biomass of 59.75 and 38.50 kJ mol$^{-1}$ for *Botryococcus* and *Hapalosiphon* respectively, assuming that the difference between the values is due to the amount of lipids contained in *Botryococcus*. On the other hand, analysis of oil extracted from original biomass shows differences between activation energies of both extracts, indicating that not only the amount of lipids affects the pyrolytic profile but also its composition. In this way, activation energy of *BB* in this study (110 kJ mol$^{-1}$) may be greater than reported by Liu et al. 2012 (59.75 kJ mol$^{-1}$) due to differences between hydrocarbon composition, since several races classify *Botryococcus braunii* according to the type of hydrocarbon produced reporting alkadienes, botryococcenes, and lycopadienes for the races A, B, and L respectively [6].

## Air Gasification Process

Using a validated model of biomass gasification, the influence of moisture content and the biomass/air equivalence ratio on the composition and heating value of producer gas was theoretically studied. In this simulation, the heat losses

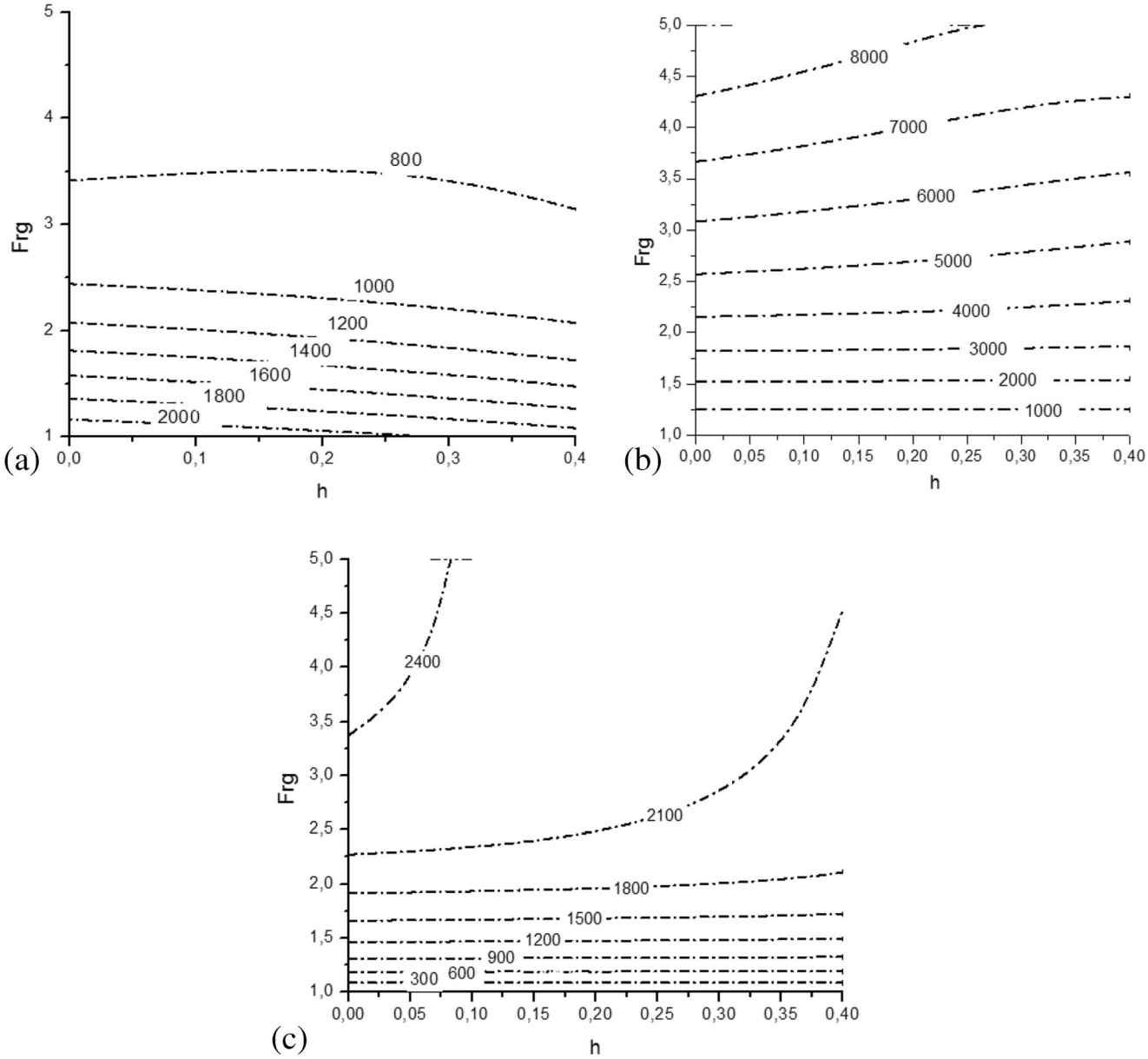


**Fig. 4** **a** Temperature distribution-K. **b** High heating value-MJ/kg. **c** Engine fuel quality-MJ/kg

were not included because the model was established to be adiabatic. Thus, the results presented in this section are related with the thermodynamic limits of the algal gasification process. Figures 4 and 5 are depicted as response surfaces, z = f(x,y), in function of the fuel-air equivalence ratio ($F_{rg}$) and biomass moisture content ($h$) as process parameters. The response variables (z) are represented in contours lines of each subfigure.

### Reaction Temperature

In Fig. 4a, it can be seen how process temperature tends to decrease when $F_{rg}$ increases. This is due to a higher amount of biomass than air. The temperature is also affected by the biomass moisture content, which can be explained due to energy needed to evaporate the water contained in the biomass [38]. Thus, if the water in biomass increases, this leads to decrease the reaction temperature and the gaseous fuel concentration decreases too.

In real conditions, the temperature of the process is critical for self-sustaining the reaction. When temperature is not high enough, it may cause the loss of autothermal condition leading to process disruption. That is, the reaction temperature decreases if fuel/air equivalence ratio increases due to the lower amount of oxygen involved in the reaction process, which avoids the release of the biomass energy in the exothermic reactions. For $F_{rg}$ greater than 3.5, the reaction temperature is about 800 K, while for fuel/air equivalence ratio higher than

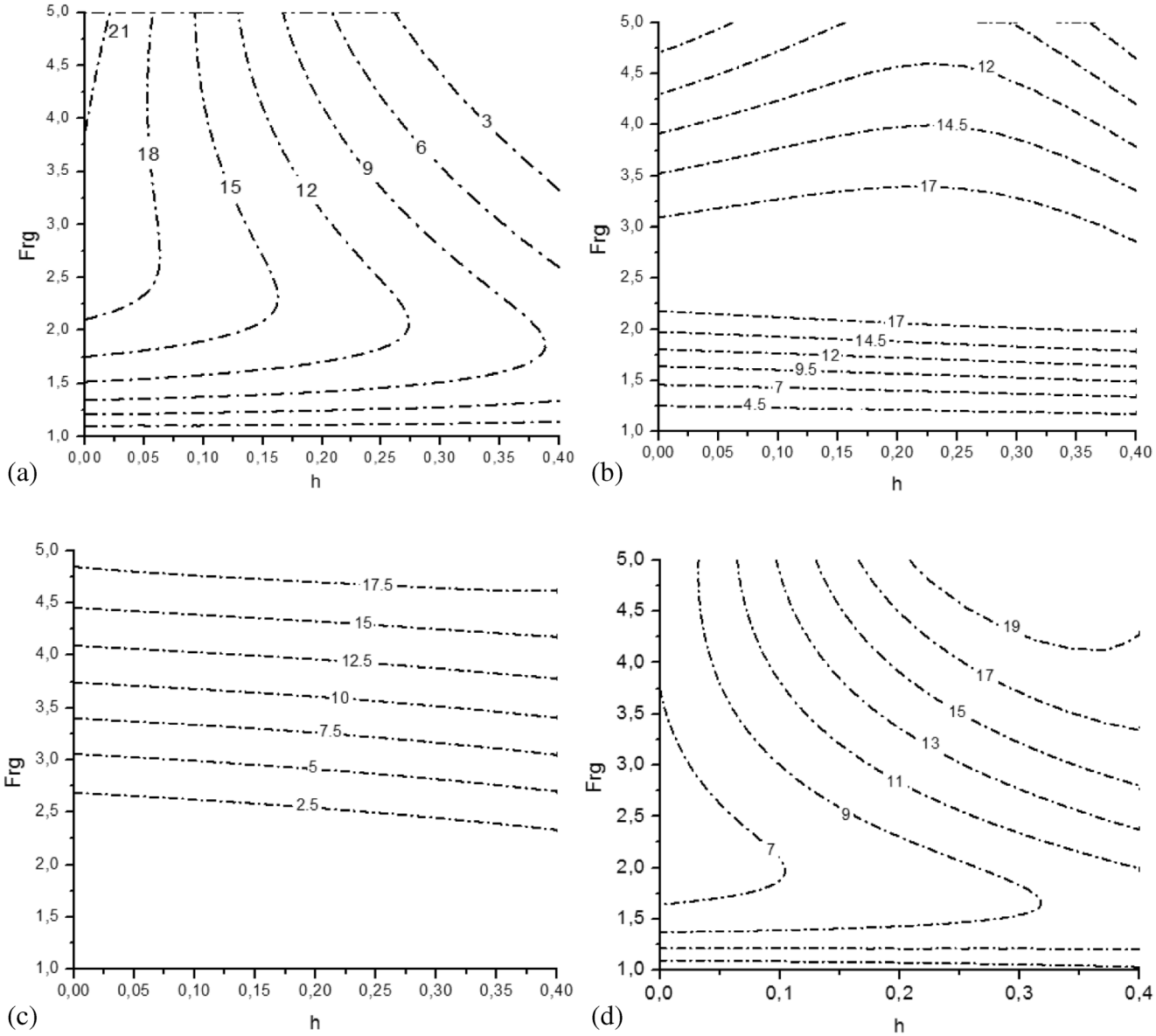


**Fig. 5** Volumetric distribution of syngas components as a function of moisture content and $F_{rg}$. **a** CO %, **b** $H_2$%, **c** $CH_4$%, **d** $CO_2$%

3.5, the process is difficult to reach due to autothermal considerations [38, 50].

The $HHV_{PG}$ tends to increase at high values of $F_{rg}$ and low moisture content because the production of gases with high heating value such as $H_2$, $CH_4$, and CO increases (Fig. 4b). However, the moisture content of the biomass is inversely related to $HHV_{PG}$. The EFQ distribution (Fig. 4c) shows a similar trend of $HHV_{PG}$ because it is a function of producer gas energy density. The highest values of EFQ are found in the intervals of highest concentration of CO and $H_2$. Under high values of humidity and $F_{rg}$, the predominant molecule is $CH_4$, which has a negative effect on EFQ when compared to the effect of CO, because methane requires more air in a stoichiometric combustion to produce the same amount of energy [38].

## Composition of the Syngas

The estimated composition of the producer gas in volumetric concentration for each gaseous species, i.e., CO(a), $H_2$(b), $CH_4$(c) y $CO_2$(d) is shown in Fig. 5. The distribution of the concentration of the gaseous species depends mainly on the chemical balance between the species, which is controlled indirectly by the reaction temperature, which in turn depends on the biomass/air ratio and the moisture content of the biomass [38].

The content of carbon monoxide (Fig. 5a) in the producer gas is affected by both $F_{rg}$ and $h$. The trend to increase its yield at low moisture content of the biomass and high values of $F_{rg}$ is due to the fact that the air content supplied is very limited and the combustion is increasingly incomplete, favoring the

production of CO. In addition, if the moisture content increases, this leads to favor the production of hydrogen and carbon dioxide due to the water gas shift reaction [38]. This result is comparable with that reported by Sanchez-Silva et al. (2013) [28], who observed higher yields of hydrogen if steam was used as gasifying agent.

The hydrogen content (Fig. 5b) is mostly affected by the change in $F_{rg}$, where values of 2.5 give a maximum yield in its content regardless of the moisture content of the biomass. This can be explained because the reaction for hydrogen production is mainly affected by the reaction temperature, which is related to the $F_{rg}$. When the biomass/air ratio increases, a point of inflection is reached in a relatively low critical temperature. This favors the production of methane instead of hydrogen [38, 51].

The methane content (Fig. 5c) increases with high $F_{rg}$ values, which are reflected in a relatively low reaction temperature. This is due to the advantage of the reaction between hydrogen and carbon monoxide to form methane [50]. These results agree with what was reported by Hirano et al. (1998) [52], who found that the fraction of $H_2$ produced in the gasification of *Spirulina* improves when the reaction temperature raises up to 1000 °C. In the simulation, this temperature was achieved at $F_{rg}$ of 3.5, a value at which a high performance in the production of hydrogen was observed in the simulation.

Regarding carbon dioxide (Fig. 5d), two behaviors are observed with respect to the process variables. In the first one, an increase in its concentration is observed when decreasing the $F_{rg}$, and this is because the gasification process approaches to the stoichiometry of the reaction, resulting in increasing $CO_2$ and water concentrations. On the other hand, a maximum yield is achieved at high values of both $F_{rg}$ and moisture content, where steam reacts with carbon monoxide to form carbon dioxide and hydrogen. The best conditions for energetic gases production are 2.5 ($F_{rg}$) and 0.05 ($h$), which give CO 18 vol.%, $H_2$ 17 vol.%, and $CH_4$ 2 vol.% as a result.

**Table 3** Algal biomass composition and gasifier performance, adapted from [52]

| | |
|---|---|
| Proximate analysis (wt.%) | |
| Volatile matter | 63.72 |
| Fixed carbon | 14.77 |
| Moisture content | 16.2 |
| Ash | 5.31 |
| Ultimate analysis (wt.% d.b) | |
| C | 45.62 |
| H | 6.17 |
| O | 44.71 |
| N | 3.26 |
| S | 0.241 |
| High heating value—$HHV_{d.b}$ (kJ $kg^{-1}$) | 18,820 |
| Substitution formula (daf) | $C_1H_{1.6036}O_{0.6478}N_{0.0605}S_{0.0023}$ |
| Gasification performance parameters | |
| Biomass power (kW) | 63.3 |
| Producer gas power (kW) | 41.5 |

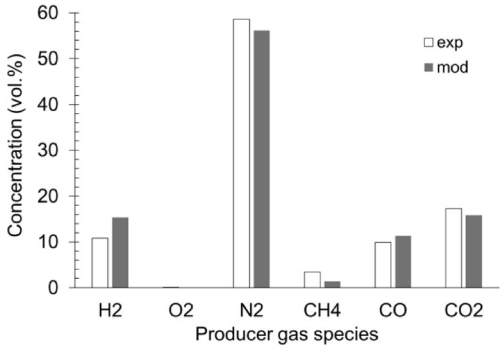


**Fig. 6** Experimental and model comparison of the producer gas composition from algal biomass gasification

## Model Validation

The response variables used to validate the gasification model as a computational tool to study and predict the energy performance of a downdraft gasifier are the composition of producer gas, fuel/air equivalence ratio $F_{rg}$, low heating value of producer gas ($LHV_{PG}$), and cold gas efficiency (CGE). The model was validated with the experimental data of Roesch [53], using different kinds of gasified biomasses in a downdraft biomass reactor at pilot scale, highlighting gasifier performance using algal biomass pellets. Table 3 presents the chemical composition of algae pellets biomass, while also presenting the gasifier operating conditions that are also used as input parameters of the model to simulate the thermochemical process. The algae pellets are made by compressing, drying, and pelletized the solids rich in carbohydrates. These pellets are a mixture of several native strains of micro-crops of *Pseudochlorococcum* sp., *Chlorococcum* sp., *Chlorella* sp., *Scenedesmus* sp., *Palmellococcus* sp., *Cylindrospermopsis* sp., and *Planktothrix* sp. [53].

Figure 6 shows the comparison of producer gas composition between experimental data (exp) and model response (mod). It a good agreement between the experimental composition and the one estimated by the model was observed. The

**Table 4** Validation of global process parameters of the algal downdraft gasification

| Parameter | Experimental results [53] | Model results | Relative error (%) |
|---|---|---|---|
| $LHV_{pg}$ (kJ $kg^{-1}$) | 2920 | 3045.19 | 4.29 |
| CGE (%) | 65.56 | 73.89 | 12.71 |
| $F_{rg}$ (−) | 2.34 | 2.10 | 10.26 |
| $T_{reaction}$ (K) | 923–1023 | 957.83 | 3.77 |

numerical results tend to overestimate CO concentration while $CO_2$ is underestimated. The $CH_4$ had a slight trend to be underestimated, and $H_2$ was slightly overestimated. The behavior shown by the model is ascribed to the auxiliary equations of the model approach (Eqs. 13 and 14). At the reaction temperature of ~ 685 °C calculated by the model for the gasification conditions of Table 3, the equilibrium constant for $H_2$ reduction with char is activated backwards (Eq. 13); therefore, production of $CH_4$ is inhibited, while $H_2$ increases. In the same way, the water gas shift reaction is also activated backwards leading to increase the CO, and consequently reducing the $CO_2$ concentration in the producer gas from the algal biomass (Eq. 14).

Nevertheless, despite the variation in producer gas composition, it is highlighted that the model adequately predicts the global values of the process performance such as producer gas heating value ($LHV_{PG}$), cold gas efficiency (CGE), fuel/air equivalence ratio ($F_{rg}$), and the reaction temperature (see Table 4).

Model accuracy to calculate the producer gas composition was analyzed and quantified using the root mean square deviation (RMSD) or root mean square error (RMSE) between model results and experimental data [42, 43]. The average root mean square error of the model respecting to the producer gas composition was found to be ± 2.4%vol. On the other hand, the model accuracy to calculate the global parameters of the gasification process is quantified by the relative error, where the average relative error of $LHV_{pg}$, CGE, $F_{rg}$, and reaction temperature is ~ 7.8%. By comparing the experimental and predicted results to determine model accuracy, it is reasonable to state that the model could be used to study the gasification of the *Botryococcus braunii* microalga in downdraft reactors under autothermal and steady conditions.

## Conclusions

The pyrolysis characteristics of microalga *Botryococcus braunii* have been studied by TGA/DTG analysis. Its pyrolysis curves could be divided into two degradation zones. Firstly, the main devolatilization step took place between 250 and 350 °C, associated to the degradation of protein and carbohydrates. The second step corresponds to lipids degradation between 380 and 480 °C. Activation energies were calculated for each conversion degree with their respectively pre-exponential factor. The average apparent activation energy was determined by two methods, Kissinger-Akahira-Sunose and Flynn-Wall-Ozaka methods, where we obtained values of 106 kJ $mol^{-1}$ and 110 kJ $mol^{-1}$ respectively in the conversion range of 20–80%. The high values of volatile material, carbon content and heating value, and low activation energy value found in *Botryococcus braunii* suggest that is an excellent raw material for thermochemical conversion pathways. The gasification model proved to be a useful tool to simulate gasification process for *Botryococcus braunii*. This allowed to predict results according to the experiential data in downdraft reactor. $H_2$ and CO were the main products in the simulated gasification process. The correct combination of variables ($h$, $F_{rg}$) leads to obtaining a syngas with high energy content, which through processes such as Fisher-Tropsch process can be transformed into liquid fuels.

**Acknowledgments** This work was supported by the Agencia Nacional de Hidrocarburos (ANH), Departamento Administrativo de Ciencia, Tecnología e Innovación Colciencias and Universidad de Antioquia, Program 721-2015 "Convocatoria para la formación de recurso humano en Colombia en el área de hidrocarburos, a través de proyectos de investigación año 2015".

## References

1. Liu G, Liao Y, Wu Y, Ma X, Chen L (2017) Characteristics of microalgae gasification through chemical looping in the presence of steam. Int J Hydrog Energy 42:22730–22742. https://doi.org/10.1016/j.ijhydene.2017.07.173
2. Alipour R, Yusup S, Uemura Y et al (2014) Syngas production from palm kernel shell and polyethylene waste blend in fluidized bed catalytic steam co-gasification process. Energy 75:40–44. https://doi.org/10.1016/j.energy.2014.04.062
3. Saidina NA, Misson M, Haron R, Ahmad M, Bunch F (2012) Bio-oils and diesel fuel derived from alkaline treated empty fruit bunch (EFB). International Journal of Biomass & Renewables 1:6–14
4. Uemura Y, Saadon S, Osman N, Mansor N, Tanoue KI (2015) Torrefaction of oil palm kernel shell in the presence of oxygen and carbon dioxide. Fuel 144:171–179. https://doi.org/10.1016/j.fuel.2014.12.050
5. López-González D, Fernandez-Lopez M, Valverde JL, Sanchez-Silva L (2014) Comparison of the steam gasification performance of three species of microalgae by thermogravimetric–mass spectrometric analysis. Fuel 134:1–10. https://doi.org/10.1016/j.fuel.2014.05.051
6. Eroglu E, Okada S, Melis A (2011) Hydrocarbon productivities in different Botryococcus strains: comparative methods in product quantification. J Appl Phycol 23:763–775. https://doi.org/10.1007/s10811-010-9577-8
7. Mata TM, Martins AA, Caetano NS (2010) Microalgae for biodiesel production and other applications: a review. Renew Sust Energ Rev 14:217–232. https://doi.org/10.1016/j.rser.2009.07.020
8. Rawat I, Ranjith Kumar R, Mutanda T, Bux F (2013) Biodiesel from microalgae: a critical evaluation from laboratory to large scale production. Appl Energy 103:444–467. https://doi.org/10.1016/j.apenergy.2012.10.004
9. Pingle SD, Landge AD (2013) Comparative account on proliferation rate of microalgae used in biodiesel production by indigenously prepared bioreactors. Journal of Advanced Laboratory Research in Biology 4(2):60–62
10. Raheem A, Wan Azlina WAKG, Taufiq Yap YH, Danquah MK, Harun R (2015) Thermochemical conversion of microalgal biomass for biofuel production. Renew Sust Energ Rev 49:990–999. https://doi.org/10.1016/j.rser.2015.04.186
11. Brown TM, Duan P, Savage PE (2010) Hydrothermal liquefaction and gasification of Nannochloropsis sp. Energy Fuel 24:3639–3646. https://doi.org/10.1021/ef100203u

12. Lopez Gonzales D, Valverde JL, Fernandez Lopez M, Sanchez Silva L (2013) Thermogravimetric-mass spectrometric analysis on combustion of lignocellulosic biomass. Bioresour Technol 143: 562–574. https://doi.org/10.1016/j.biortech.2013.06.052
13. Di Blasi C (2009) Combustion and gasification rates of lignocellulosic chars. Prog Energy Combust Sci 35:121–140. https://doi.org/10.1016/j.pecs.2008.08.001
14. Vo TK, Ly HV, Lee OK, Lee EY, Kim CH, Seo JW, Kim J, Kim SS (2017) Pyrolysis characteristics and kinetics of microalgal Aurantiochytrium sp. KRS101. Energy 118:369–376. https://doi.org/10.1016/j.energy.2016.12.040
15. López-González D, Fernandez-Lopez M, Valverde JL, Sanchez-Silva L (2014) Pyrolysis of three different types of microalgae: kinetic and evolved gas analysis. Energy 73:33–43. https://doi.org/10.1016/j.energy.2014.05.008
16. Shuping Z, Yulong W, Mingde Y, Chun L, Junmao T (2010) Pyrolysis characteristics and kinetics of the marine microalgae Dunaliella tertiolecta using thermogravimetric analyzer. Bioresour Technol 101:359–365. https://doi.org/10.1016/j.biortech.2009.08.020
17. Li D, Chen L, Zhang X, Ye N, Xing F (2011) Pyrolytic characteristics and kinetic studies of three kinds of red algae. Biomass Bioenergy 35:1765–1772. https://doi.org/10.1016/j.biombioe.2011.01.011
18. Bui HH, Tran KQ, Chen WH (2015) Pyrolysis of microalgae residues—a kinetic study. Bioresour Technol 199:362–366. https://doi.org/10.1016/j.biortech.2015.08.069
19. Simas-Rodrigues C, Villela HDM, Martins AP, Marques LG, Colepicolo P, Tonon AP (2015) Microalgae for economic applications: advantages and perspectives for bioethanol. J Exp Bot 66: 4097–4108. https://doi.org/10.1093/jxb/erv130
20. Domozych DS, Ciancia M, Fangel JU, Mikkelsen MD, Ulvskov P, Willats WGT (2012) The cell walls of green algae: a journey through evolution and diversity. Front Plant Sci 3:82. https://doi.org/10.3389/fpls.2012.00082
21. Barneto AG, Vila C, Ariza J (2011) Eucalyptus kraft pulp production: thermogravimetry monitoring. Thermochim Acta 520:110–120. https://doi.org/10.1016/j.tca.2011.03.027
22. Yang H, Yan R, Chen H, Lee DH, Zheng C (2007) Characteristics of hemicellulose, cellulose and lignin pyrolysis. Fuel 86:1781–1788. https://doi.org/10.1016/j.fuel.2006.12.013
23. Wang S, Hu Y, Bernard B et al (2017) Pyrolysis mechanisms of typical seaweed polysaccharides. J Anal Appl Pyrolysis 124:373–383
24. De Lasa H, Salaices E, Mazumder J, Lucky R (2011) Catalytic steam gasification of biomass: catalysts, thermodynamics and kinetics. Chem Rev 111:5404–5433
25. Balat M, Balat M, Kırtay E, Balat H (2009) Main routes for the thermo-conversion of biomass into fuels and chemicals. Part 2: Gasification systems. Energy Convers Manag 50:3158–3168. https://doi.org/10.1016/j.enconman.2009.08.013
26. Tiong L, Komiyama M, Uemura Y, Thanh T (2016) Catalytic supercritical water gasification of microalgae: comparison of Chlorella vulgaris and Scenedesmus quadricauda. J Supercrit Fluids 107:408–413. https://doi.org/10.1016/j.supflu.2015.10.009
27. Sikarwar VS, ZHao M, Fennell PS, et al (2017) Progress in biofuel production from gasification. Prog Energy Combust Sci 61:189–248. https://doi.org/10.1016/j.pecs.2017.04.001
28. Sanchez Silva L, López González D, Garcia Minguillan AM, Valverde JL (2013) Pyrolysis, combustion and gasification characteristics of Nannochloropsis gaditana microalgae. Bioresour Technol 130:321–331. https://doi.org/10.1016/j.biortech.2012.12.002
29. Yang X, Zhang R, Fu J, Geng S, Cheng JJ, Sun Y (2014) Pyrolysis kinetic and product analysis of different microalgal biomass by distributed activation energy model and pyrolysis-gas chromatography-mass spectrometry. Bioresour Technol 163:335–342. https://doi.org/10.1016/j.biortech.2014.04.040
30. Duman G, Uddin MA, Yanik J (2014) Hydrogen production from algal biomass via steam gasification. Bioresour Technol 166:24–30. https://doi.org/10.1016/j.biortech.2014.04.096
31. Shi S, Zhou X, Chen W et al (2017) Thermal and kinetic behaviors of fallen leaves and waste tires using thermogravimetric analysis. Bioresource 12:4707–4721
32. Perez JF, Melgar A, Tinaut FV (2014) Modeling of fixed bed downdraft biomass gasification: application on lab-scale and industrial reactors. Int J Energy Res 38:319–338
33. Arbelaez AA (2019) Analysis, modeling and improvement of production process of the microalga Botryococcus braunii for energy purposes. Master thesis. University of Antioquia, 2019
34. Bligh E, Dyer W (1959) A rapid method of total lipid extraction and purification. Can J Biochem Physiol 37:911–917
35. Ceylan S, Kazan D (2015) Pyrolysis kinetics and thermal characteristics of microalgae Nannochloropsis oculata and Tetraselmis sp. Bioresour Technol 187:1–5. https://doi.org/10.1016/j.biortech.2015.03.081
36. Kissinger H (1957) Reaction kinetics in differential thermal analysis. Anal Chem 29:1702–1706
37. Flynn J, Wall L (1966) A quick, direct method for the determination of activation energy from thermogravimetric data. J Polym Sci 4: 323–328
38. Melgar A, Perez JF, Laget H, Horillo A (2007) Thermochemical equilibrium modelling of a gasifying process. Energy Convers Manag 48:59–67. https://doi.org/10.1016/j.enconman.2006.05.004
39. Pérez JF, Melgar A, Horrillo A (2016) Thermodynamic methodology to support the selection of feedstocks for decentralised downdraft gasification power plants. Int J Sustainable Energy 36:1010–1028. https://doi.org/10.1080/14786451.2016.1162792
40. Barrera R, Salazar C, Pérez JF (2014) Thermochemical equilibrium model of synthetic natural gas production from coal gasification using Aspen Plus. Int J Chem Eng 14:1–18. https://doi.org/10.1155/2014/192057
41. Campanella A, Muncrief R, Harold MP, Griffith DC, Whitton NM, Weber RS (2012) Thermolysis of microalgae and duckweed in a $CO_2$-swept fixed-bed reactor: bio-oil yield and compositional effects. Bioresour Technol 109:154–162. https://doi.org/10.1016/j.biortech.2011.12.115
42. Rizzo AM, Prussi M, Bettucci L, Libelli IM, Chiaramonti D (2013) Characterization of microalga Chlorella as a fuel and its thermogravimetric behavior. Appl Energy 102:24–31. https://doi.org/10.1016/j.apenergy.2012.08.039
43. Liu Y, Lim LRX, Wang J, et al (2012) Investigation on pyrolysis of microalgae Botryococcus braunii and Hapalosiphon sp. Ind Eng Chem Res 51:10320–10326. https://doi.org/10.1021/ie202799e
44. Li D, Chen L, Zhang X et al (2010) Evaluation of the pyrolytic and kinetic characteristics of Enteromorpha prolifera as a source of renewable bio-fuel from the Yellow Sea of China. Chem Eng Res Des 88:647–652
45. Wang S, Hu Y, He Z, et al (2017) Study of pyrolytic mechanisms of seaweed based on different components (soluble polysaccharides, proteins, and ash). J Renewable Sustainable Energy 9:023102.1–12. https://doi.org/10.1063/1.4978345
46. Metzger P, Largeau C (2005) Botryococcus braunii: a rich source for hydrocarbons and related ether lipids. Appl Microbiol Biotechnol 66:486–496. https://doi.org/10.1007/s00253-004-1779-z
47. Liu YQ, Lim LRX, Wang J, Yan R, Mahakhant A (2012) Investigation on pyrolysis of microalgae botryococcus braunii and Hapalosiphon sp. Ind Eng Chem Res 51:10320–10326. https://doi.org/10.1021/ie202799e
48. Wu K, Liu J, Wu Y, Chen Y, Li Q, Xiao X, Yang M (2014) Pyrolysis characteristics and kinetics of aquatic biomass using

thermogravimetric analyzer. Bioresour Technol 163:18–25. https://doi.org/10.1016/j.biortech.2014.03.162

49. Yuan T, Tahmasebi A, Yu J (2015) Comparative study on pyrolysis of lignocellulosic and algal biomass using a thermogravimetric and a fixed-bed reactor. Bioresour Technol 175:333–341. https://doi.org/10.1016/j.biortech.2014.10.108
50. Henriksen U, Ahrenfeldt J, Jensen TK, Gøbel B, Bentzen JD, Hindsgaul C, Sørensen LH (2006) The design, construction and operation of a 75 kW two-stage gasifier. Energy 31:1542–1553. https://doi.org/10.1016/j.energy.2005.05.031
51. Tian T, Li Q, He R, Tan Z, Zhang Y (2017) Effects of biochemical composition on hydrogen production by biomass gasification. Int J Hydrog Energy 42:19723–19732. https://doi.org/10.1016/j.ijhydene.2017.06.174
52. Hirano A, Hon-nami K, Kunito S et al (1998) Temperature effect on continuous gasification of microalgal biomass: theoretical yield of methanol production and its energy balance. Catal Today 45:399–404
53. Roesch H (2011) Downdraft gasification of various biomass feedstocks for energy production. Master thesis. Florida State University, 2011. Retrieved from http://purl.flvc.org/fsu/fd/FSU_migr_etd-5146